


Article

# Chemical Conversion of Hardly Ionizable Rhenium Aryl Chlorocomplexes with *p*-Substituted Anilines

Martin Štícha <sup>1,\*</sup> , Ivan Jelínek <sup>2</sup> and Mikuláš Vlk <sup>2</sup><sup>1</sup> Department of Chemistry, Faculty of Science, Charles University, 12000 Prague 2, Czech Republic<sup>2</sup> Department of Analytical Chemistry, Faculty of Science, Charles University, 12000 Prague 2, Czech Republic; ijelinek@natur.cuni.cz (I.J.); mikulas.vlk@natur.cuni.cz (M.V.)

\* Correspondence: sticha@natur.cuni.cz

**Abstract:** Fast and selective analytical methods help to ensure the chemical identity and desired purity of the prepared complexes before their medical application, and play an indispensable role in clinical practice. Mass spectrometry, despite some limitations, is an integral part of these methods. In the context of mass spectrometry, specific problems arise with the low ionization efficiency of particular analytes. Chemical derivatization was used as one of the most effective methods to improve the analyte's response and separation characteristics. The Schotten–Baumann reaction was successfully adapted for the derivatization of ESI hardly ionizable Re(VII) bis(catechol) oxochloro complex. Various alkyl and halogen *p*-substituted anilines as possible derivatization agents were tested. Unlike the starting complex, the reaction products were easily ionizable in electrospray, providing structurally characteristic molecular and fragment anions. DFT computer modeling, which proposed significant conformation changes of prepared complexes within their deprotonation, proved to have a close link to MS spectra. High-resolution MS and MS/MS measurements complemented with collision-induced dissociation experiments for detailed specification of prepared complexes' fragmentation pathways were used. The specified fragmentation schemes were analogous for all studied derivatives, with an exception for [Re(O)(Cat)<sub>2</sub>PIPA].

**Keywords:** high-resolution mass spectrometry; rhenium complexes; chemical derivatization; coordination chemistry; DFT



**Citation:** Štícha, M.; Jelínek, I.; Vlk, M. Chemical Conversion of Hardly Ionizable Rhenium Aryl Chlorocomplexes with *p*-Substituted Anilines. *Molecules* **2021**, *26*, 3427. <https://doi.org/10.3390/molecules26113427>

Academic Editors: Alessandra Boschi and Petra Martini

Received: 29 April 2021

Accepted: 1 June 2021

Published: 5 June 2021

**Publisher's Note:** MDPI stays neutral with regard to jurisdictional claims in published maps and institutional affiliations.



**Copyright:** © 2021 by the authors. Licensee MDPI, Basel, Switzerland. This article is an open access article distributed under the terms and conditions of the Creative Commons Attribution (CC BY) license (<https://creativecommons.org/licenses/by/4.0/>).

## 1. Introduction

In analytical chemistry, derivatization is primarily used to modify an analyte that cannot be analyzed by a particular analytical method or to improve selectivity. Chemical derivatization helps to improve separation characteristics and the sensitivity of detection [1]. Chemical derivatization has played an important role in GC/MS analysis, where derivatization is used to increase volatility, change the analyte's ionization properties, or affect analyte fragmentation [2]. The most commonly used derivatives in GC/MS are methyl, ethyl, acetyl, or silyl esters of fatty acids. Mostly in situ derivatization methods are used, where the sample preparation and chemical modification take place in one step. Derivatization in liquid chromatography has a different rationale and, therefore, different rules apply when selecting reagents [3]

The goal of chemical derivatization in ESI/MS is to convert the poorly ionizable or non-ionizable substance into an easily detectable one by changing its chemical and physical properties. ESI is considered very sensitive toward polar compounds. However, for low polarity or non-polar compounds it has been considered less satisfactory than APCI. Substances that form ions in a solution are generally well ionizable by ESI. In contrast, APCI is more suitable for ionizing low to medium polar substances containing atoms with high proton affinity [4]. Although ESI/MS is one of the most efficient analytical methods, its use in detecting some low polar rhenium complexes is limited. Problems with the ionization of these molecules are caused by the absence of acidic or basic groups in the structure. The

analyte can be chemically modified to increase ionization efficiency by introducing groups capable of protonation or deprotonation [5–17].

The derivatization potential for ESI-MS in analytical chemistry has been presented in numerous publications [7,8,10,16–22]. One of the disadvantages of derivatization is the possibility of affecting not only the target analyte but also other components of the sample. The Schotten–Baumann reaction (SB reaction) is a commonly used procedure for the derivatization of primary, secondary, and tertiary amines in GC/NPD, GC/FPD, and GC/MS. Various alkyl chloroformates as derivatizing agents have been tested for these purposes; their utilization in aqueous solutions and two-phase solvent solutions have been reported and reviewed [23–25]. Aniline and its substituents are among the simplest weak bases that are highly susceptible to electrophilic and nucleophilic substitutions as the basis of SB reactions. For chloro- and bromo-substituted derivatives, a characteristic isotope pattern can be successfully used to identify fragments. This is why these substances have been chosen as potential derivatizing agents to analyze non-ionizable rhenium complexes. The resulting derivative contains a nitrogen atom as an easily ionizable group and improves the ionization efficiency of the analytes by ESI.

Recently, we showed the suitability of MS for structure characterization of  $\text{Re}^{\text{V, VI, VII}}$  complexes with aromatic bidentate ligands [26]. Although MS provided useful structural information in a series of observed reaction and degradation products, we have occasionally met hardly ionizable structural types [27]. Namely,  $\text{Re}^{\text{VII}}$  oxochloro catechol complex resisted against ionization under ESI, APCI, and APPI conditions. We found an immediate solution in a reaction with *p*-bromoaniline and assumed this reaction worthwhile for further investigation and optimization. This contribution aims to systematically investigate the possibility of chemical conversion of bis(1,2-dihydroxybenzen)-chloro-oxorhenium complex to ESI ionizable products via reactions with aniline and its *p*-substituted derivatives (*p*-chloroaniline, *p*-bromoaniline, *p*-isopropylaniline, *p*-toluidine). The time-course of the derivatization reaction was followed both by ESI/MS and UV-Vis kinetic measurements. Collision-induced dissociation experiments revealed typical fragmentation pathways of formed molecular anions.

## 2. Results and Discussion

### 2.1. Chemistry

The hardly ionizable Chlorocomplexes  $[\text{Re}^{\text{VII}}(\text{O})\text{Cl}(\text{Cat})_2]$  were prepared using a procedure that was adapted from [26]. One equivalent (4.4 mg) of tetrabutylammonium tetrachlorooxorhenate(V)  $[(\text{n-Bu}_4\text{-N})(\text{ReOCl}_4)]$  was dissolved in 1.5 mL of acetonitrile. Two equivalents of ligand 1,2-dihydroxybenzene and two equivalents of triethylamine (10% (*v/v*) solution in acetonitrile) were added and the reaction mixture was stirred for 3 days at laboratory temperature. Since catechol ligand lacks the free dissociable group, the yielding compound remains uncharged and its structural characterization by MS is impossible. Its presence in the reaction mixture was presumed entirely from a similarity between absorption spectra describing the formation of deprotonated pyrogallol analog. However, its ESI-MS structure identification is possible after the reaction with aniline (Figure 1), yielding an ESI ionizable reaction product [27].

Derivatives were prepared by mixing 10  $\mu\text{L}$  of the reaction mixture described above with 50  $\mu\text{L}$  of *p*-substituted aniline (5% (*v/v*) solution in acetonitrile). The reaction scheme of derivatization is shown in Figure 1. All prepared complexes are described in Table 1. For full chemical names see Table S6 in the Supplementary Materials.

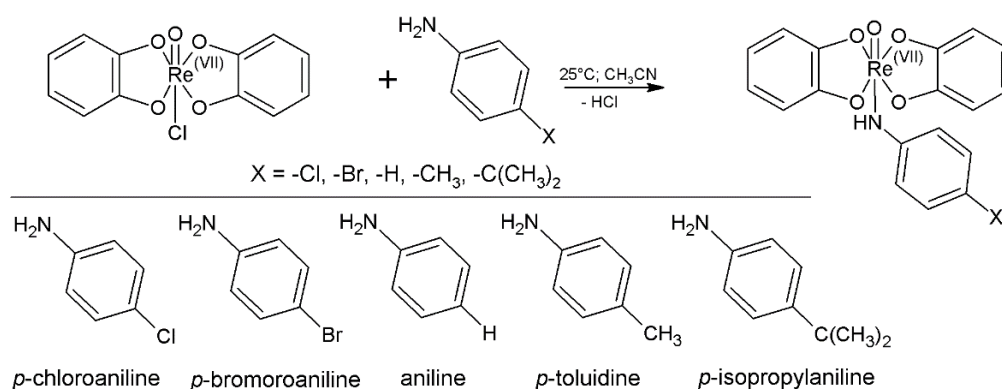


**Figure 1.** Derivatization reaction of uncharged rhenium(VII) chlorocomplexes with *p*-substituted aniline.

**Table 1.** Labels and formulas of prepared rhenium complexes.

Entry	X	Complex	Formula
1	Cl	[Re <sup>VII</sup> (O)(Cat) <sub>2</sub> PClA] <sup>−a</sup>	C <sub>18</sub> H <sub>12</sub> ClNO <sub>5</sub> Re
2	Br	[Re <sup>VII</sup> (O)(Cat) <sub>2</sub> PBrA] <sup>−a</sup>	C <sub>18</sub> H <sub>12</sub> BrNO <sub>5</sub> Re
3	H	[Re <sup>VII</sup> (O)(Cat) <sub>2</sub> An] <sup>−a</sup>	C <sub>18</sub> H <sub>13</sub> NO <sub>5</sub> Re
4	CH <sub>3</sub>	[Re <sup>VII</sup> (O)(Cat) <sub>2</sub> PT] <sup>−a</sup>	C <sub>19</sub> H <sub>15</sub> NO <sub>5</sub> Re
5	C(CH <sub>3</sub> ) <sub>2</sub>	[Re <sup>VII</sup> (O)(Cat) <sub>2</sub> PIPA] <sup>−a</sup>	C <sub>21</sub> H <sub>19</sub> NO <sub>5</sub> Re

<sup>a</sup> Deprotonated ion.

## 2.2. Molecular Modeling

Density functional theory could be a possible MS/MS prediction tool useful in structure elucidating. Molecular modeling proposed the significant change of molecular conformation of studied aniline derivatives before and after ionization. We illustrate the structures of neutral and deprotonated [Re(O)(Cat)<sub>2</sub>PBrA] in Figure 2.

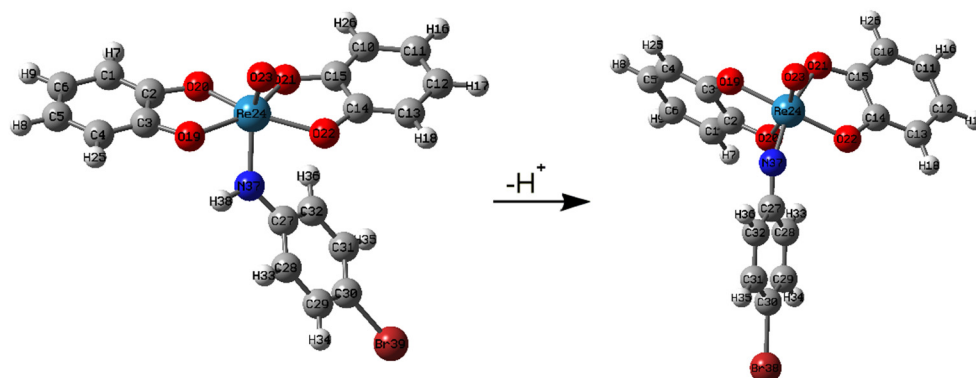


**Figure 2.** The DFT calculated structures of neutral and deprotonated [Re(O)(Cat)<sub>2</sub>PBrA].

Evident is the shortening of the Re-N bond in the course of deprotonation. As it results from more detailed modeling, the shortening of the Re-N bond is accompanied by the prolongation of the Re-O(20) bond in a ligand, the increase in the Re-N-C(22) angle, and the decrease in the dihedral angle C(14)-O(22)-Re-O(19). For details, see the corresponding computation data in the Supplementary Materials. The extent of such structural changes depends on the aromatic substituent linked via derivatization. The decisive element here seems to be the basicity of the aniline derivative entering the SB reaction. The bar graph showing the correlation between Re-N bond shortening and the basicity of the used aniline derivative is shown in Figure 3. The pK<sub>a</sub> values of used aniline derivatives were obtained from [28].

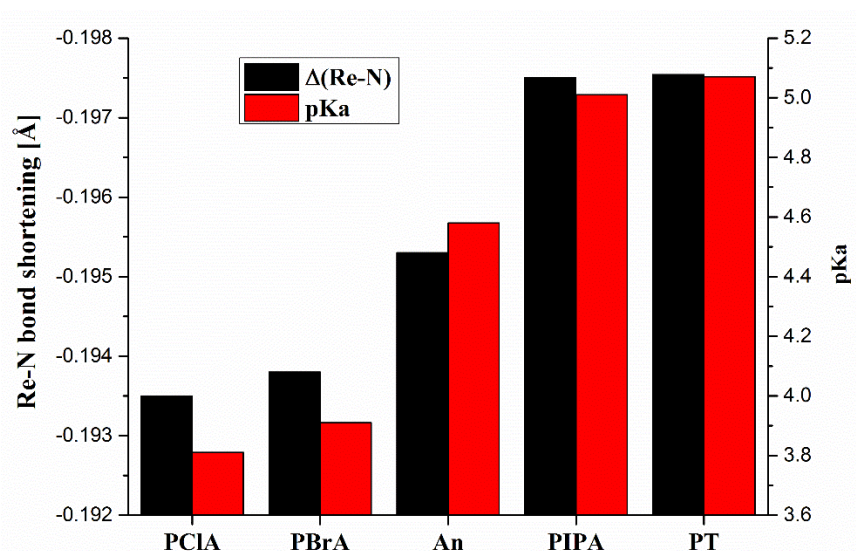


**Figure 3.** Correlation between Re-N bond shortening  $\Delta(\text{Re-N})$  and pKa of *p*-substituted anilines; PCIA-*p*-chloroaniline, PBrA-*p*-bromoaniline, An-aniline, PIPA-*p*-isopropylaniline, PT-*p*-toluidine.

### 2.3. High-Resolution Mass Spectrometry Characterization

All molecular ions of prepared derivatives exhibit characteristic isotopic distributions. We compared the similarity between the calculated and experimental molecular ion isotopic patterns using the similarity index (SI) [29]. The [(1-SI) 100] values given in Table 2 indicate an apparent coincidence between the calculated and experimental spectra and the correct assignment of the elemental composition to the  $m/z$  values of the observed ions.

**Table 2.** Theoretical and experimental exact masses of molecular anions of studied derivatives. The error values express the difference between theoretical and experimental masses; the similarity index expresses the resemblance between theoretical and experimental isotope patterns of molecular anions.

Entry	Molecular Formula	Theoretical $m/z$	Measured $m/z$	Error (mDa)	Error (ppm)	(1-SI) 100 (%)
$[\text{Re}(\text{O})(\text{Cat})_2\text{PCIA}]^-$	$\text{C}_{18}\text{H}_{12}\text{ClNO}_5\text{Re}$	543.9958	543.9969	-1.1	-2.0	98.6
$[\text{Re}(\text{O})(\text{Cat})_2\text{PBrA}]^-$	$\text{C}_{18}\text{H}_{12}\text{BrNO}_5\text{Re}$	587.9445	587.9440	0.4	0.8	94.2
$[\text{Re}(\text{O})(\text{Cat})_2\text{An}]^-$	$\text{C}_{18}\text{H}_{13}\text{NO}_5\text{Re}$	510.0357	510.0360	-0.3	-0.6	98.1
$[\text{Re}(\text{O})(\text{Cat})_2\text{PT}]^-$	$\text{C}_{19}\text{H}_{15}\text{NO}_5\text{Re}$	524.0514	524.0507	0.7	1.2	89.2
$[\text{Re}(\text{O})(\text{Cat})_2\text{PIPA}]^-$	$\text{C}_{21}\text{H}_{19}\text{NO}_5\text{Re}$	552.0827	552.0828	-0.2	-0.3	98.1

Excellent agreement between the isotope pattern calculated and that obtained by MS of the  $[\text{Re}(\text{O})(\text{Cat})_2\text{PBrA}]^-$  complex is documented in Figure 4. An analogous satisfactory agreement of exact mass and isotopic distribution for all other derivatives was observed.

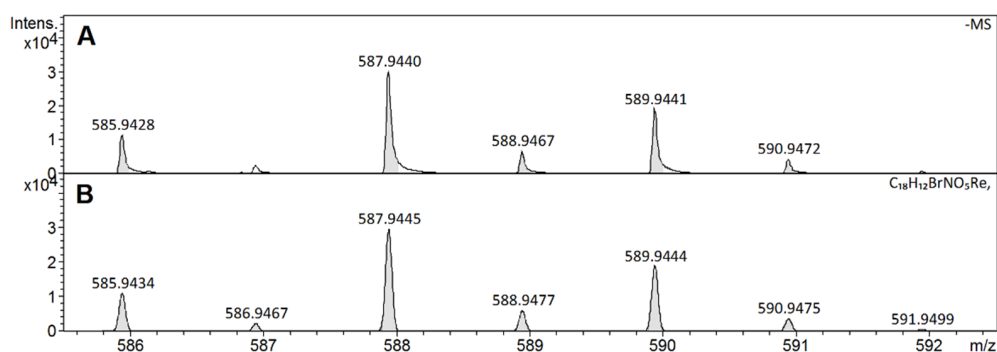


**Figure 4.** Experimental (A) and calculated (B) isotope pattern of  $[\text{Re}(\text{O})(\text{Cat})_2\text{PBrA}]^-$ .

#### 2.4. Reaction Time-Course

A significant color change accompanies the reaction of the  $[\text{Re}^{\text{VII}}(\text{O})\text{Cl}(\text{Cat})_2]$  complex with the aniline derivative. Therefore, UV-Vis absorption spectrophotometry can be applied for the evaluation of its reaction rate. The major absorption band at  $\lambda_{\text{max}} = 630$  nm and the minor one at  $\lambda_{\text{max}} = 390$  nm characterize the intensive blue-green coloration of the  $[\text{Re}^{\text{VII}}(\text{O})\text{Cl}(\text{Cat})_2]$  complex. The product of the reaction with the aniline derivative is pale yellow, showing an absorption maximum at 355 nm. The rate of the derivatization reaction with *p*-bromoaniline was followed by the UV/Vis absorption measurement. The corresponding spectra recorded at defined time intervals are shown in Figure 5. A decrease of more than 90% over the 15 min interval was observed for the absorption band at  $\lambda_{\text{max}} = 630$  nm. The proportional decrease in the height of the related absorption band at  $\lambda_{\text{max}} = 390$  nm was observed. After 50 min, both absorption maxima disappear in favor of a minor absorption band at  $\lambda_{\text{max}} = 355$  nm (see inset).

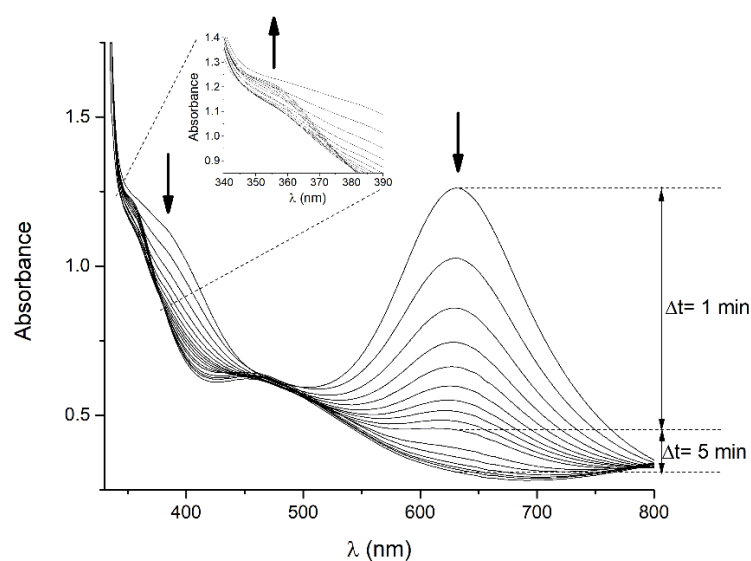


**Figure 5.** UV/Vis kinetics of derivatization reaction of uncharged  $[\text{Re}^{\text{VII}}(\text{O})\text{Cl}(\text{Cat})_2]$  chlorocomplex with *p*-bromoaniline.

An alternative insight into the mechanism of derivatization reaction has been provided by complementary ESI/MS kinetic measurement displayed in Figure 6. The intensity of ion  $m/z$  588 (red line), as the desired derivatization product, achieves a maximum at approximately 15 min. This is consistent with the observed rate of the decrease in the  $[\text{Re}^{\text{VII}}(\text{O})\text{Cl}(\text{Cat})_2]$  absorption band ( $\lambda_{\text{max}} = 630$  nm). The appearance of ion  $m/z$  454 (blue line) revealed another function of aniline derivative acting as a weakly basic accelerator of the  $\text{Re}^{\text{V}}$  complex oxidation to a higher  $\text{Re}^{\text{VI}}$  form. Therefore, we can observe a decrease in the intensity of peak  $m/z$  419 (black line) due to the slow transformation of complex  $[\text{Re}^{\text{V}}(\text{O})(\text{Cat})_2]^-$  present in the reaction mixture. As the  $\text{Re}^{\text{VI}}$  complex species are prone to further oxidation, the intensity of ion  $m/z$  454, reaching a maximum within 15 min, decreases at a moderate rate.

The time-course of ionic intensities helps to reveal the actual structure of ion  $m/z$  454. Although the high-resolution MS data are available, there is still uncertainty about the exact structure of ion  $m/z$  454, where both  $[\text{Re}^{\text{VI}}(\text{O})\text{Cl}(\text{Cat})_2]^-$  and the adduct with chlorine  $[\text{Re}^{\text{VII}}(\text{O})(\text{Cat})_2]\text{Cl}^-$  fit in the same mass. We believe that the shape of the time dependence of the ionic intensities presented in Figure 6 precludes the presence of a chlorine adduct.



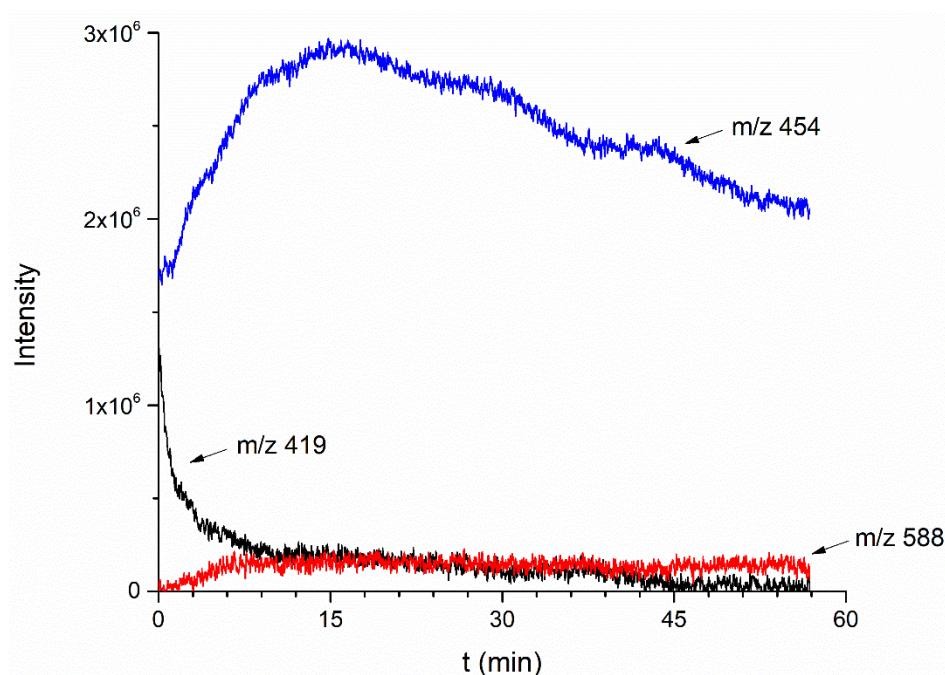


**Figure 6.** ESI-MS kinetics of derivatization reaction of uncharged  $[\text{Re}^{\text{VII}}(\text{O})\text{Cl}(\text{Cat})_2]$  chlorocomplex with *p*-bromoaniline.

### 2.5. Collision Induced Dissociation (CID)

The tandem mass spectrometry at 35eV collision energy in negative ionization mode was used to determine the structure of the prepared derivatives. The obtained MS/MS spectrum in Table 3 is very simple. The accurate mass measurement indicates that the main peak  $m/z$  480 is formed by the loss of catechol moiety from the precursor marked by the blue diamond. It is evident that the isotopic profile retains the distribution confirming the presence of rhenium and bromine isotopes. It is even possible to observe the loss of the aromatic ring from the other catechol moiety to form ion M-2L  $m/z$  404. Fragmentation behavior suggested the presence of a remarkably strong Re-N bond. On the other hand, the ion  $m/z$  327 is formed by the loss of substituted aniline and the whole process ends in  $\text{ReO}_4^-$  and  $\text{ReO}_3^-$  ions resp. Since the same behavior was observed for almost all prepared complexes, the fragmentation pattern was demonstrated in this example only. The proposed fragmentation pathway is presented in Figure 7. High mass-accuracy measurements according to Table 3 and fragmentation patterns allowed us to identify the structure of all prepared derivatives.

**Table 3.** Theoretical and experimental masses of  $[\text{Re}(\text{O})(\text{Cat})_2\text{PBrA}]$  CID fragment ions measured at collision energy 35 eV. The error values express the difference between theoretical and experimental masses.

Nom. $m/z$	Ion Formula	Theoretical $m/z$	Measured $m/z$	Error (mDa)	Error (ppm)	Rel. Abundance (%)
588	$\text{C}_{18}\text{H}_{12}\text{BrNO}_5\text{Re}^-$	587.9462	587.9459	0.5	0.3	0.3
480	$\text{C}_{12}\text{H}_8\text{BrNO}_3\text{Re}^-$	479.9233	479.9271	-7.9	-3.8	-3.8
404	$\text{C}_6\text{H}_4\text{BrNO}_3\text{Re}^-$	403.892	403.8931	-2.8	-1.1	-1.1
327	$\text{C}_6\text{H}_4\text{O}_4\text{Re}^-$	326.9673	326.9681	-2.5	-0.8	-0.8
251	$\text{ReO}_4^-$	250.936	250.9354	2.3	0.6	0.6
235	$\text{ReO}_3^-$	234.9411	234.9383	11.7	2.8	2.8

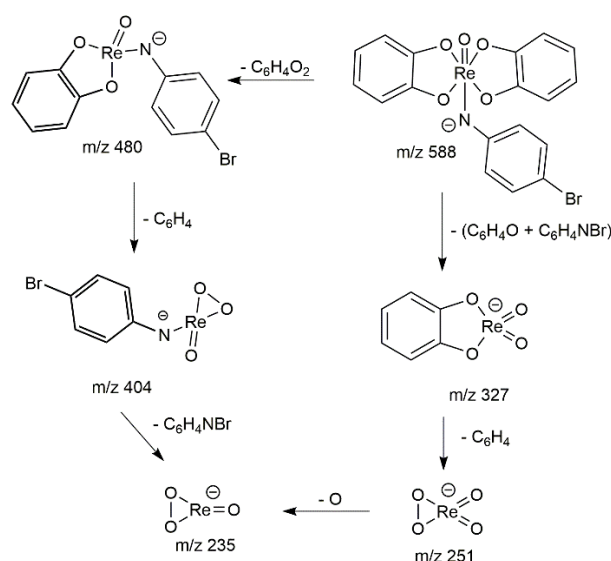


Figure 7. Fragmentation scheme of  $[\text{Re}(\text{O})(\text{Cat})_2\text{PBrA}]$ .

According to the collision-induced dissociation results in Figure 8, it can be seen that the intensity of the product ion formed by the loss of one catechol ligand M-L ( $m/z$  480) reaches a maximum at the same collision energy as the ion formed by simultaneous fragmentation of substituted aniline ( $m/z$  327), but the intensity of this ion is only around 10% relative to the major peak. This is consistent with the observed shortening of the Re-N bond.

The green curve on the CID diagram describing the formation of the ion  $m/z$  251 does not exhibit a significant maximum, and it is evident that the formation of that ion corresponds to different processes. The spotting of this ion already at zero collision energy can be attributed to the decomposition of the complex; for example, by air humidity. Another mechanism of  $m/z$  251 ion formation is the loss of the aromatic ring from  $m/z$  327. Dissociation of the Re-N bond and cleavage of aniline from the  $m/z$  404 ion occurs only at high CE.

Calculated significant deformation of the molecule, which should be linked both with the shortening of the Re-N bond and the prolongation of a Re-O(20) bond (approximately 0.2 Å) in a single ligand, has an experimental consequence in CID experiments. Such a bond is going to be the most easily fragmented, yielding ion  $m/z$  480. The intensity of the simultaneously arising ion  $m/z$  327 is then significantly lower due to the lower energetical convenience of such fragmentation pathway. As expected, the ion on the favorable fragmentation pathway has the highest negative energy. The difference in energies is about 177 kcal mol<sup>-1</sup> in favor of ion  $m/z$  480. The energy differences were converted from Hartrees into kcal mol<sup>-1</sup> using a conversion factor of 627.5.

The fragmentation of all prepared complexes was analogous. The data are available in the Supplementary Materials (Figures S1–S12). We observed the only exception for  $[\text{Re}(\text{O})(\text{Cat})_2\text{PIPA}]^-$ . Here, the different behavior is not related to the change of bond length but the product stability of arising ions. As is evident from the corresponding CID diagram (Figure 8B), a significant shift to higher collision energies has been observed for the ion  $\text{ReO}_3^-$ . The collision energy where the ion  $m/z$  235 reaches a maximum is almost 40 eV or 3.2 eV regarding  $E_{\text{CM}}$  higher. Unlike the other complexes, the  $\text{ReO}_3^-$  ion ( $m/z$  235) in a  $[\text{Re}(\text{O})(\text{Cat})_2\text{PIPA}]^-$  fragmentation pathway is not formed directly from ion M-2L but through the ion  $m/z$  325 as an intermediate. Ion  $m/z$  325 is formed by a loss of the methane molecule (Figure 9), where aryl-vinyl stabilization due to  $\pi$  electrons conjugation takes part. Such types of stabilization are unique for  $[\text{Re}(\text{O})(\text{Cat})_2\text{PIPA}]^-$  and not possible for other prepared complexes. We calculated that the difference in energies of the fragments with and without aryl-vinyl stabilization is around 48 kcal mol<sup>-1</sup>. The elemental composition of

ion  $m/z$  325 was verified using HRMS. We have obtained the exact mass of 351.9993 Da by measuring, while the calculated value for  $C_8H_7NO_3Re^-$  is 351.9989 Da. It means the error is  $-1.0$  ppm.

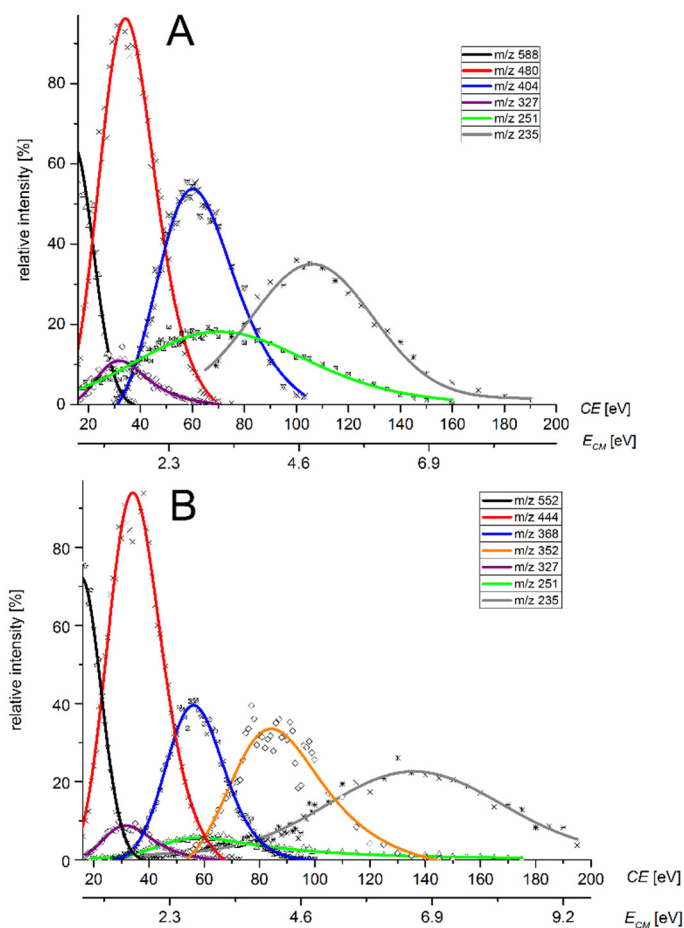


**Figure 8.** CID diagram of the dependence of the relative intensity of fragmented ions on the collision energy: (A)  $[Re(O)(Cat)_2PBrA]^-$  (B)  $[Re(O)(Cat)_2PIPA]^-$ .

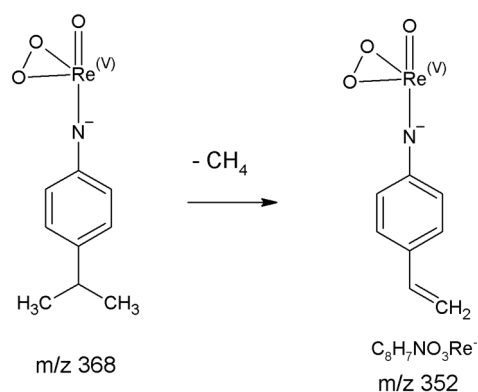


**Figure 9.** Proposed fragmentation mechanism of ion M-2L yielding from  $[Re(O)(Cat)_2PIPA]$  complex.

### 3. Materials and Methods

#### 3.1. Materials and Reagents

Tetrabutylammonium tetrachlorooxorhenate(V), 4-Chloroaniline, 4-Bromoaniline, 4-Methylaniline, 4-isopropylaniline, aniline, 4-Methylcatechol, and 1,2-dihydroxybenzene were purchased from Sigma-Aldrich. Acetonitrile (HPLC grade) and triethylamine were



purchased from Fisher Scientific. Nitrogen used as nebulizing and drying gas was generated by MS-NGM 11 (Bruker Daltonics, Bremen, Germany) nitrogen generator.

### 3.2. Instrumentation and Software

ESI/MS experiments were conducted on a Bruker QqTOF compact instrument operated using Compass otofControl 4.0 (Bruker Daltonics, Bremen, Germany) software. Compass DataAnalysis 4.4 (Build 200.55.2969) (Bruker Daltonics, Bremen, Germany) software was used for data processing. Molecular structures and fragmentation schemes were drawn using ChemDraw (PerkinElmer Informatics, Waltham, MA, USA). Isotope patterns and exact masses of ions were calculated using IsotopePattern 3.0 (Build 201.9.27) (Bruker Daltonics, Bremen, Germany) utility. Analytical scales Kern ALJ 220-4 (Kern & Sohn, Balingen, Germany) were used to weigh solids. Stirring procedures were performed using a Stuart SA8 (Cole Parmer, UK) stirrer.

ESI/MS data were collected in negative ion mode at scan range from  $m/z$  50 to  $m/z$  1000. The temperature of the drying gas was set to 220 °C at 3.0 L min<sup>-1</sup> flow rate. Cone voltage was 2800 V. Samples were injected into the nebulizer by a syringe pump (Cole Parmer, USA) at a flow rate 3  $\mu$ L min<sup>-1</sup>.

Time-based ESI/MS measurement was performed by mixing the reactants in concentrated form and diluting the reaction mixture right before the ESI ion source using the second syringe pump with acetonitrile.

The isolation width of parent ions in CID experiments was set to 5 Da, the pressure of collision gas (nitrogen) in the collision cell was  $2.5 \times 10^{-3}$  mbar. Measurements were conducted in the range from 10 eV to 200 eV collision energy (ELAB) with a step of 1 eV. Mass spectrometer was calibrated using clusters of ammonium formate. OriginPro 9.0 was used for fitting CID dependences.

Agilent 8453 spectrophotometer (Agilent, Santa Clara, CA, USA) was used for UV/Vis kinetic measurements. Spectra were recorded at 0.1 nm resolution from 330 to 750 nm and processed with UV-Visible Chemstation (Agilent, Santa Clara, CA, USA).

### 3.3. DFT Calculation

Optimizations of molecular geometries and other theoretical calculations were performed at the density functional level of theory (DFT B3LYP) using Gaussian 16 [30] and LanL2DZ basis set. Both non-ionized and ionized forms of studied complexes were optimized, and frequency calculations were performed with optimized structures at the same level of theory.

## 4. Conclusions

The Schotten–Baumann (SB) reaction has been successfully adapted for the derivatization of MS hardly ionizable Re(VII) chlorocomplexes. We systematically studied the reaction of the Re(VII) bis(catechol) chlorocomplex with the set of halogen and alkyl anilines as derivatization agents. The SB reaction products are easily ionizable under common ESI conditions providing structurally characteristic molecular and fragment anions. Based on DFT computation, the effect of Re-N bond shortening in the course of complex deprotonation was simulated and also correlated with the basicity of aniline derivative used as a derivatization agent. Our conclusions follow the known relation between the basicity of the reaction environment and the yield of the SB reaction. However, an attempt to increase the yield of the derivatization reaction by adding triethylamine (TEA) to the reaction mixture was unsuccessful. Such a conclusion probably refers to the fast reaction providing the dioxorhenium complex as a competition to the SB reaction itself.

The shortening of the Re-N bond throughout neutral molecule deprotonation and concurrent prolongation of Re-O(20) makes the cleavage of one or both ligands the most probable initial fragmentation pathway of studied complexes, leading to the formation of abundant M-L and M-2L anions.

Although the fragmentation of all studied complexes was analogous, we observed a notable difference concerning the formation of  $\text{ReO}_3^-$  ( $m/z$  235) ion in a fragmentation scheme of  $[\text{Re}(\text{O})(\text{Cat})_2\text{PIPA}]^-$ . Unlike the other complexes, this ion is not formed directly from an M-2L fragment but through an aryl-vinyl stabilized unique  $m/z$  325, unseen in other studied complexes' fragmentation schemes.

**Supplementary Materials:** The following are available online, Figures S1–S13 and Tables S1–S7. Figure S1. HR ESI–MS/MS spectra of complex 1; collision energy, CE, was 40 eV, Figure S2. HR ESI–MS/MS spectra of complex 2; collision energy, CE, was 40 eV, Figure S3. HR ESI–MS/MS spectra of complex 3; collision energy, CE, was 40 eV, Figure S4. HR ESI–MS/MS spectra of complex 4; collision energy, CE, was 40 eV, Figure S5. HR ESI–MS/MS spectra of complex 5; collision energy, CE, was 40 eV, Figure S6. Pro-posed fragmentation scheme of complex 1, Figure S7. Proposed fragmentation scheme of complex 3, Figure S8. Proposed fragmentation scheme of complex 4, Figure S9. Proposed fragmentation scheme of complex 5, Figure S10. CID diagram of complex 1, Figure S11. CID diagram of complex 3, Figure S12. CID diagram of complex 4. Figure S13. Graph of calculated bond elongation of prepared complexes. Table S1. Cartesian coordinates calculated for the optimized neutral structure of complex 1, Table S2. Cartesian coordinates calculated for the optimized neutral structure of complex 2, Table S3. Cartesian coordinates calculated for the optimized neutral structure of complex 3, Table S4. Cartesian coordinates calculated for the optimized neutral structure of complex 4, Table S5. Cartesian coordinates calculated for the optimized neutral structure of complex 5, Table S6. Chemical names, labels, and formulas of prepared rhenium complexes, Table S7. Calculated bond elongation of prepared complexes.

**Author Contributions:** M.Š. conceived, designed and performed the experiments; M.Š. and I.J. wrote the paper; M.V. was responsible for data analysis and visualization. All authors have read and agreed to the published version of the manuscript.

**Funding:** Financial support from Charles University Centre of Advanced Materials (CUCAM) (OP VVV Excellent Research Teams, project number CZ.02.1.01/0.0/0.0/15\_003/ 0000417) is greatly acknowledged.

**Institutional Review Board Statement:** Not applicable.

**Informed Consent Statement:** Not applicable.

**Data Availability Statement:** Data is contained within the article or Supplementary Materials.

**Conflicts of Interest:** The authors declare no conflict of interest.

**Sample Availability:** Samples of the compounds mentioned in the materials section are available from the authors.

## Abbreviations

electrospray ionization (ESI); atmospheric pressure photoionization (APPI); atmospheric pressure chemical ionization (APCI); high-resolution mass spectrometry (HRMS); tandem mass spectrometry (MS/MS); gas chromatography/mass spectrometry (GC/MS); gas chromatography/nitrogen phosphorous detector (GC/NPD); gas chromatography/flame photometric detector (GC/FPD); collision-induced dissociation (CID); density functional theory (DFT).

## References

1. Anderegg, R.J. Derivatization in mass spectrometry: Strategies for controlling fragmentation. *Mass Spectrom. Rev.* **1988**, *7*, 395–424. [[CrossRef](#)]
2. Eggink, M.; Wijnmans, M.; Ekkebus, R.; Lingeman, H.; De Esch, I.J.P.; Kool, J.; Niessen, W.M.A.; Irth, H. Development of a Selective ESI-MS Derivatization Reagent: Synthesis and optimization for the analysis of aldehydes in biological mixtures. *Anal. Chem.* **2008**, *80*, 9042–9051. [[CrossRef](#)]
3. Blau, K.; King, G.S. Chapter 2–3. In *Handbook of Derivatives for Chromatography*; Heyden & Son Ltd.: London, UK, 1977.
4. Niessen, W.M.A. State-of-the-art in liquid chromatography–mass spectrometry. *J. Chromatogr. A* **1999**, *856*, 179–197. [[CrossRef](#)]
5. Zaikin, V.G.; Halket, J.M. Derivatization in mass spectrometry—7. On-line derivatization/degradation. *Eur. J. Mass Spectrom.* **2006**, *12*, 79–115. [[CrossRef](#)] [[PubMed](#)]

6. Van Berkel, G.J.; Asano, K.G. Electrospray as a controlled current electrolytic cell—Electrochemical ionization of neutral analytes for detection by electrospray mass-spectrometry. *Anal. Chem.* **1994**, *66*, 2096–2102. [[CrossRef](#)]
7. Quirke, J.M.E.; Van Berkel, G.J.; Adams, C.L. Chemical Derivatization for Electrospray Ionization Mass Spectrometry. 1. Alkyl Halides, Alcohols, Phenols, Thiols, and Amines. *Anal. Chem.* **1994**, *66*, 1302–1315. [[CrossRef](#)]
8. Van Berkel, G.J.; Quirke, J.M.E.; Tigani, R.A.; Dilley, A.S.; Covey, T.R. Derivatization for electrospray ionization mass spectrometry. 3. Electrochemically ionizable derivatives. *Anal. Chem.* **1998**, *70*, 1544–1554. [[CrossRef](#)] [[PubMed](#)]
9. Niessen, W.M.A. *Liquid Chromatography-Mass Spectrometry*, 2nd ed.; Marcel Dekker: New York, NY, USA, 1999.
10. Gao, S.; Zhang, Z.P.; Karnes, H.T. Sensitivity enhancement in liquid chromatography/atmospheric pressure ionization mass spectrometry using derivatization and mobile phase additives. *J. Chromatogr. B Anal. Technol. Biomed. Life Sci.* **2005**, *825*, 98–110. [[CrossRef](#)]
11. Ming Ng, K.; Ling Ma, N.; Wai Tsang, C. Differentiation of isomeric polyaromatic hydrocarbons by electrospray Ag(I) cationization mass spectrometry. *Rapid Commun. Mass Spectrom.* **2003**, *17*, 2082–2088. [[CrossRef](#)]
12. Frenking, G.; Fröhlich, N. The Nature of the Bonding in Transition-Metal Compounds. *Chem. Rev.* **2000**, *100*, 717–774. [[CrossRef](#)]
13. Nikolova-Damyanova, B. Retention of lipids in silver ion high-performance liquid chromatography: Facts and assumptions. *J. Chromatogr. A* **2009**, *1216*, 1815–1824. [[CrossRef](#)] [[PubMed](#)]
14. Nikolova-Damyanova, B.; Momchilova, S. Silver ion HPLC for the analysis of positionally isomeric fatty acids. *J. Liq. Chromatogr. Relat. Technol.* **2002**, *25*, 1947–1965. [[CrossRef](#)]
15. Momchilova, S.; Nikolova-Damyanova, B. Stationary phases for silver ion chromatography of lipids: Preparation and properties. *J. Sep. Sci.* **2003**, *26*, 261–270. [[CrossRef](#)]
16. Bayer, E.; Gfrörer, P.; Rentel, C. Coordination-Ionspray-MS (CIS-MS), a Universal Detection and Characterization Method for Direct Coupling with Separation Techniques. *Angew. Chem. Int. Ed.* **1999**, *38*, 992–995. [[CrossRef](#)]
17. Moriwaki, H. Electrospray ionization mass spectrometric detection of low polar compounds by adding NaAuCl<sub>4</sub>. *J. Mass Spectrom.* **2016**, *51*, 1096–1102. [[CrossRef](#)]
18. Van Berkel, G.J.; Quirke, J.M.E.; Adams, C.L. Derivatization for electrospray ionization-mass spectrometry. 4. Alkenes and alkynes. *Rapid Commun. Mass Spectrom.* **2000**, *14*, 849–858. [[CrossRef](#)]
19. Johnson, D.W. Contemporary clinical usage of LC/MS: Analysis of biologically important carboxylic acids. *Clin. Biochem.* **2005**, *38*, 351–361. [[CrossRef](#)] [[PubMed](#)]
20. Higashi, T.; Shimada, K. Derivatization of neutral steroids to enhance their detection characteristics in liquid chromatography-mass spectrometry. *Anal. Bioanal. Chem.* **2004**, *378*, 875–882. [[CrossRef](#)] [[PubMed](#)]
21. Honda, A.; Hayashi, S.; Hifumi, H.; Honma, Y.; Tanji, N.; Iwasawa, N.; Suzuki, Y.; Suzuki, K. MPAI (Mass Probes Aided Ionization) Method for Total Analysis of Biomolecules by Mass Spectrometry. *Anal. Sci.* **2007**, *23*, 11–15. [[CrossRef](#)]
22. Van Berkel, G.J.; McLuckey, S.A.; Glish, G.L. Charge determination of product ions formed from collision-induced dissociation of multiply protonated molecules via ion molecule reactions. *Anal. Chem.* **1991**, *63*, 2064–2068. [[CrossRef](#)]
23. Zaikin, V.G.; Halket, J.M. Derivatization in mass spectrometry—2. Acylation. *Eur. J. Mass Spectrom.* **2003**, *9*, 421–434. [[CrossRef](#)] [[PubMed](#)]
24. Hušek, P. Chloroformates in gas chromatography as general purpose derivatizing agents. *J. Chromatogr. B* **1998**, *717*, 57–91. [[CrossRef](#)]
25. Kataoka, H. 2.1.2—Gas Chromatography of Amines as Various Derivatives. *Journal of Chromatography Library* **2005**, *70*, 364–404. [[CrossRef](#)]
26. Štícha, M.; Jelínek, I.; Poláková, J.; Kaliba, D. Characterization of Rhenium(V) Complexes with Phenols Using Mass Spectrometry with Selected Soft Ionization Techniques. *Anal. Lett.* **2015**, *48*, 2329–2342. [[CrossRef](#)]
27. Sticha, M.; Jelínek, I.; Kaliba, D.; Polakova, J. Analytical study of rhenium complexes with pyrogallol and catechol. *Chem. Pap.* **2017**, *71*, 819–830. [[CrossRef](#)]
28. Williams, R. pKa Data Compiled by R. Williams. Available online: [https://organicchemistrydata.org/hansreich/resources/pka/pka\\_data/pka-compilation-williams.pdf](https://organicchemistrydata.org/hansreich/resources/pka/pka_data/pka-compilation-williams.pdf) (accessed on 28 April 2021).
29. Wan, K.X.; Vidavsky, I.; Gross, M.L. From similarity index to spectral contrast angle. *J. Am. Soc. Mass Spectrom.* **2002**, *13*, 85–88. [[CrossRef](#)]
30. Frisch, M.J.; Trucks, G.W.; Schlegel, H.B.; Scuseria, G.E.; Robb, M.A.; Cheeseman, J.R.; Scalmani, G.; Barone, V.; Mennucci, B.; Petersson, G.A.; et al. *Gaussian 16, Revision C.01*; Gaussian Inc.: Wallingford, CT, USA, 2016.